ARTICLE IN PRESS

Journal of Computational and Applied Mathematics ▮ (▮▮▮▮) ▮▮▮–▮▮▮

Contents lists available at ScienceDirect

Journal of Computational and Applied Mathematics

journal homepage: www.elsevier.com/locate/cam

Radial basis function simulation of slow-release permanganate for groundwater remediation via oxidation

G. Yao [a,*], K.M. Bliss [b], M. Crimi [c], K.R. Fowler [a], J. Clark-Stone [a], W. Li [a], P.J. Evans [d]

[a] Department of Mathematics, Clarkson University, Potsdam, NY 13699-5815, United States
[b] Department of Applied Mathematics, Virginia Military Institute, Lexington, Lexington, VA 24450, United States
[c] Institute for a Sustainable Environment, Clarkson University, Potsdam NY 13699-5715, United States
[d] CDM Smith Inc., 14432 SE Eastgate Way, Suite 100, Bellevue, WA 98007, United States

ARTICLE INFO

Article history:
Received 30 July 2015
Received in revised form 5 February 2016

Keywords:
Radial basis function
Contaminant
Reactive transport
Chemical oxidation

ABSTRACT

An emerging strategy for remediation of contaminated groundwater is the use of permanganate cylinders for contaminant oxidation. The cylinders, which are only a few inches in diameter, can be placed in wells or pushed directly into the subsurface. This work focuses on the modeling and simulation of the reactive process to better understand the design of a group of cylinders for large scale contaminated sites. The underlying model is a coupled system of nonlinear partial differential equations accounting for advection, dispersion, and reactive transport for a contaminant and the permanganate in two spatial dimensions. Radial Basis Functions collocation method is used to simulate different spatial arrangements of the cylinders to understand the behavior of the system and gain insight into designing a remediation strategy for a large-scale contaminated region. Since the radial basis function collocation method is a meshless method, the locations of the cylinders are not tied to a numerical grid, making it an attractive choice for determining optimal placement. Our focus is to (1) identify a domain of influence measuring the effectiveness of the injected cylinders, (2) understand the placement for multiple cylinders required to effectively clean-up a given domain, and (3) determine a protocol for injecting multiple cylinders over time. We provide numerical results showing that domain of influence is a way to measure the effectiveness of installed cylinders. Domain of influence of one through three sources are simulated. Placement of two cylinders for an area of 13*ft* by 3*ft* and three sources for an area of 26*ft* by 6*ft* are sufficient to clean the contaminant within a reasonable time period. The average concentrations of oxidant and contaminant are simulated for the cases of a third cylinder is installed at different time and locations.

1. Introduction

In Situ Chemical Oxidation (ISCO) with permanganate (MnO_4^-) is a common technology used to treat contaminated groundwater. ISCO is the delivery of chemical oxidants, typically via injection, to groundwater to degrade contaminants. One challenge with traditional ISCO is the rapid dissolution and reaction of the oxidant in the environment. Often, the oxidant concentration is very high immediately after injection, but decreases rapidly over time due to reaction with reduced

* Corresponding author.
E-mail address: gyao@clarkson.edu (G. Yao).

http://dx.doi.org/10.1016/j.cam.2016.02.006
0377-0427/

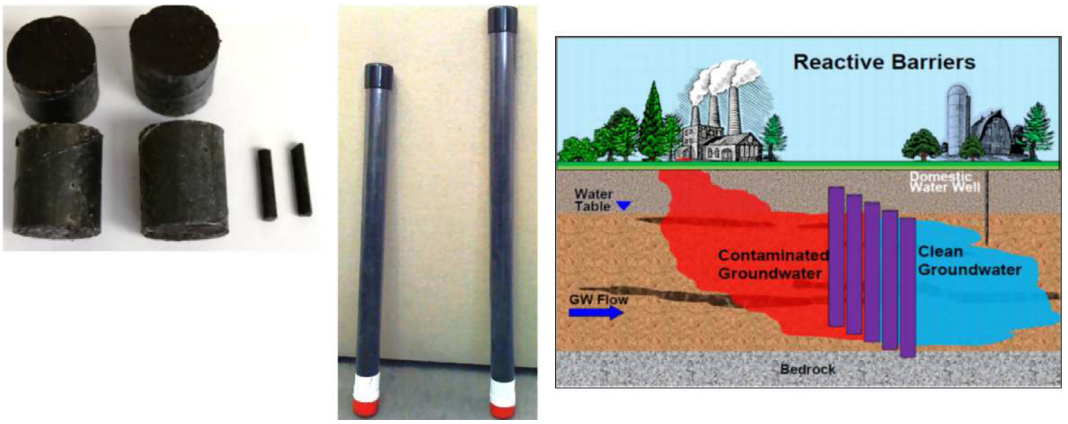

Fig. 1. MnO_4^- cylinders and their use in the field courtesy of Carus Corporation.

subsurface constituents, which is referred to as natural oxidant demand (NOD). Many injections typically need to be used in succession to fully treat a contaminated site, thereby driving up costs [1]. Also, there are several design challenges for ISCO (and other technologies involving delivery of liquid amendments). The first challenge occurs when a heterogeneous contaminated site contains finer textured soils that do not accept liquid injections. When this happens, the chemical will flow through the more permeable layers because this path offers the least resistance.

An approach to address these challenges is through the use of a encapsulated passive, slow-release oxidant, which is inserted and allowed to dissolve and intercept the contaminant over numerous years. Encapsulation prevents instant dissolution of the entire oxidant mass into the environment [2–4,1,5,6]. Studies have been conducted by Kang et al. [4] on the most effective, least reactive coating. They determined that paraffin wax polymer can best extend the oxidation lifespan. Some benefits of paraffin wax include that it is an environmentally benign product, it is safe to work with, it is solid at ambient temperatures, and it is insoluble in water. Its insolubility in water ensures that the oxidant contained within the shell is shielded from nonproductive use.

The first Slow Release Permanganate Cylinders (SRPCs) were manufactured in 2007. Now they are commercially available and manufactured through Carus Corporation, see Fig. 1. The cylinders can be installed in new or existing vertical and horizontal wells or installed using direct push technology. They can be vertically stacked and installed horizontally next to each other to cover the width and depth of a contaminant plume. Much headway has already been made towards the modeling of oxidant release into groundwater.

Mathematical modeling and simulation can be used to gain insight into the design of remediation strategies. Reactive transport models have found increased application in recent years in porous media [7,8]. This kind of models aims to provide reaction and transport dynamics of multicomponent system [9,8]. Early studies developed the theoretical basis of such models and necessary numerical tools to solve them. Some applications to problems of reactive contaminant transport in groundwater and flow through reacting hydrothermal systems are introduced in [10,11]. Work was conducted by Wolf (2013) [12] and Slaugh (2015) [13] to develop a slow-release oxidant design tool focused on the release of oxidant from cylinders and its reactive transport in 1-D. The tool was based on the analytical solutions to two interactive chemical unsaturated groundwater flow models. Laboratory data were used to verify the oxidant release term. The tool was developed in Microsoft Excel, which was used because of its universal acceptance and its ease-of-use (Wolf, 2013) [12]. A draw back in [12] is the restriction to one spatial dimension since the lateral interaction between cylinders was not considered.

In this paper, the reaction between MnO_4^- and a single contaminant in an ISCO diffusion–transport reaction model is simulated by a system of coupled partial differential equations in two-dimensional space. Radial basis function collocation method (RBFCM) is used to simulate different spatial arrangements of the injection points when planning the system. RBFCM is a method that uses scattered points in domains and the function values at the points to approximate solutions to PDEs. Mesh and numerical integration are not needed in the discretization process. The first RBFCM was introduced by Kansa in 1990 [14]. Since then, RBFCM have been widely used for solving various kinds of science and engineering problems, including heat transfer [15], porous media flow [16], the classical De Vahl Davis natural convection problem [17] etc. [18–20]. The main attraction of RBFCM is its effectiveness in dealing with high dimensional problems and complicated domains.

To the best of our knowledge, the earliest application of radial basis function (RBF) to groundwater problems is in 2002 [21]. The authors applied RBFCM to a steady state problem and a single linear transport equation in 2D and 3D. Since then, many researchers applied meshless methods to groundwater modeling problems to overcome the difficulties from other numerical techniques such as the finite difference methods, the finite volume method, the finite element method and others [22,23]. The focus of this work is to apply RBFCM to a coupled system of transient nonlinear PDEs in groundwater problems. An oxidant source term is included to represent the slow release of the oxidation cylinder. There are more complex and robust cases of applications of RBF collocation method on nonlinear system of PDEs that have been previously reported in the literature. For example, [24] focuses on numerical performance of RBF method on different kinds of PDEs. [25] focuses

Please cite this article in press as: G. Yao, et al., Radial basis function simulation of slow-release permanganate for groundwater remediation via oxidation, Journal of Computational and Applied Mathematics (2016), http://dx.doi.org/10.1016/j.cam.2016.02.006

on application of a local RBF method on a biomedical numerical simulations. This paper aims to find the domain of influence of oxidant cylinder for groundwater remediation, which is an specific application of RBF methods on proposed model with realistic oxidant source term.

Ultimately, the design of a chemical oxidation strategy requires determining the number and locations of cylinders in a contaminated region as well as when to change out ineffective cylinders over time. Practitioners are furthermore interested in the associated costs involved in cleaning up a contaminated site, which depends on the performance of the remediation system. The purpose of this study is to develop a numerical approach to aid in the design of large-scale remediation systems. The simulation tool aids in identifying the zone of influence of a cylinder under various physical subsurface conditions as well as insight into the interaction of multiple cylinders within a certain region. Numerical simulation of solutions to a system of diffusion–reaction–advection PDEs with experimental point source reported in [12] is utilized. The use of radial basis function on such kind of equations is not new, except the point source term is from realistic data. The purpose of the paper is not to develop a new technique for the model nor investigating numerical solution techniques of such kind PDEs. We aim to define a domain of influence of the oxidant released from the cylinder from the experimental data, and seek insight on scheduling replacement and new installation locations of the cylinders. We proceed by describing the physical models for reactive transport in groundwater flow in Section 2, give an overview of RBFCM in Section 3, and then present the test problems and numerical simulations in Section 4. We conclude and point the way towards future work in Section 5.

2. Reactive transport in groundwater model

Contaminant and oxidant interaction in saturated groundwater flow can be modeled with coupled advection–dispersion equations given by

$$\frac{R\partial C^1}{\partial t} = D_x\frac{\partial^2 C^1}{\partial x^2} + D_y\frac{\partial^2 C^1}{\partial y^2} - \nabla\cdot\mathbf{v}C^1 - kC^1C^2 + f_{release}(x,y,t), \tag{1}$$

$$\frac{R\partial C^2}{\partial t} = D_x\frac{\partial^2 C^2}{\partial x^2} + D_y\frac{\partial^2 C^2}{\partial y^2} - \nabla\cdot\mathbf{v}C^2 - kC^1C^2, \tag{2}$$

where C^1 is the oxidant (MnO_4^-) and C^2 is the contaminant. Furthermore, R is a retardation factor, $\mathbf{v}$ is the velocity, k is a second order reaction rate for the interaction of the contaminant and oxidant, and D_x and D_y as dispersion coefficients in the x and y directions. The source term is defined by

$$f_{release}(x,y,t) = \begin{cases} s(t), & \text{if } (x,y) \text{ in the cylinder,} \\ 0, & \text{otherwise} \end{cases} \tag{3}$$

and $s(t)$ which is released oxidant at the source (cylinders). Lee and Schwartz [1,26] simulate MnO_4^- release $f_{release}$ that captures the release of a solid via diffusion from a finite-height controlled release matrix of cylindrical form, described by an analytical differential equation model by Roseman and Higuchi [27]. In this study, the release of oxidant from cylinders is modeled in [12].

For this study, we assume the domain is the rectangle given by $[0, L_x] \times [0, L_y]$ with flow from left to right. In this case, the velocity component in the x direction is constant and is 0 in the y component so that the advective terms in Eqs. (1) and (2) simplify to:

$$\frac{R\partial C^1}{\partial t} = D_x\frac{\partial^2 C^1}{\partial x^2} + D_y\frac{\partial^2 C^1}{\partial y^2} - v_x\frac{\partial C^1}{\partial x} - kC^1C^2 + f_{release}, \tag{4}$$

$$\frac{R\partial C^2}{\partial t} = D_x\frac{\partial^2 C^2}{\partial x^2} + D_y\frac{\partial^2 C^2}{\partial y^2} - v_x\frac{\partial C^2}{\partial x} - kC^1C^2, \tag{5}$$

with boundary conditions for C^1 and C^2

$$\left.\frac{\partial C^1}{\partial x}\right|_{x=L_x} = 0, \qquad \left.\frac{\partial C^2}{\partial x}\right|_{x=L_x} = 0, \tag{6}$$

$$C^1(0,y,t) = 0, \qquad C^2(0,y,t) = \hat{C^2}, \tag{7}$$

$$v_yC^1 - D_y\left.\frac{\partial C^1}{\partial y}\right|_{y=0} = 0, \qquad v_yC^2 - D_y\left.\frac{\partial C^2}{\partial y}\right|_{y=0} = 0, \tag{8}$$

$$v_yC^1 - D_y\left.\frac{\partial C^1}{\partial y}\right|_{y=L_y} = 0, \qquad v_yC^2 - D_y\left.\frac{\partial C^2}{\partial y}\right|_{y=L_y} = 0, \tag{9}$$

where (6) allows for default outflow of the contaminant from the domain. Since we assume the cylinders are the only source of oxidant in the region, we impose a zero boundary condition for oxidant. A constant source of contaminant at the left hand boundary of the region is proposed since we assume contaminant continues to flow in to the region from left to right.

Please cite this article in press as: G. Yao, et al., Radial basis function simulation of slow-release permanganate for groundwater remediation via oxidation, Journal of Computational and Applied Mathematics (2016), http://dx.doi.org/10.1016/j.cam.2016.02.006

3. RBFCM

In this section, we introduce the explicit time stepping method and RBFCM to numerically solve the proposed model.

3.1. Explicit time-stepping method for general diffusion equation

We will first consider the following general nonlinear reaction transport equation in 2D

$$\frac{\partial u(\mathbf{x}, t)}{\partial t} = D_x \frac{\partial^2 u(\mathbf{x}, t)}{\partial x^2} + D_y \frac{\partial^2 u(\mathbf{x}, t)}{\partial y^2} - v_x \frac{\partial u(\mathbf{x}, t)}{\partial x} + f(\mathbf{x}, t, u(\mathbf{x}, t)) \tag{10}$$

for all $\mathbf{x}$ in a closed spatial domain Ω, and for time t, where $u(\mathbf{x}, t)$ is the concentration at the point $\mathbf{x}$ and time t. The source function $f(\mathbf{x}, t, u)$ is known.

We denote the time step by Δt, and define the grid in the time direction by $t_m = m\Delta t$, where $m \in \mathbb{N}$. Throughout this section, we discuss current and previous time steps in relation to each other; when referring to two consecutive time steps, t_m and t_{m-1}, t_m is referred to as 'current', while t_{m-1} is referred to as 'previous'. For $t_{m-1} < t \le t_m$, we approximate u and its derivatives using a one-step difference scheme, i.e., the values of $u(\mathbf{x}, t)$, $\partial u(\mathbf{x}, t)/\partial x$, $\partial u(\mathbf{x}, t)/\partial y$, $\partial^2 u(\mathbf{x}, t)/\partial x^2$, and $\partial^2 u(\mathbf{x}, t)/\partial y^2$ in the interval $(t_{m-1}, t_m]$ are determined by the value at the previous time step, t_{m-1}. For sufficiently small Δt,

$$\frac{\partial u(\mathbf{x}, t)}{\partial t} = \frac{u(\mathbf{x}, t_m) - u(\mathbf{x}, t_{m-1})}{\Delta t} + \mathcal{O}(\Delta t). \tag{11}$$

Then (10) can be approximated by

$$\frac{\hat{u}_m - \hat{u}_{m-1}}{\Delta t} = D_x \frac{\partial^2 \hat{u}_{m-1}}{\partial x^2} + D_y \frac{\partial^2 \hat{u}_{m-1}}{\partial y^2} - v_x \frac{\partial \hat{u}_{m-1}}{\partial x} + f\left(\mathbf{x}, t, \hat{u}_{m-1}\right) \tag{12}$$

where $\hat{u}_{m-1} = \hat{u}(\mathbf{x}, t_{m-1})$ and $\hat{u}_m = \hat{u}(\mathbf{x}, t_m)$ are approximations to $u(\mathbf{x}, t_{m-1})$ and $u(\mathbf{x}, t_m)$. The above equation can be rewritten as

$$\hat{u}_m = \hat{u}_{m-1} + \Delta t D_x \frac{\partial^2 \hat{u}_{m-1}}{\partial x^2} + \Delta t D_y \frac{\partial^2 \hat{u}_{m-1}}{\partial y^2} - \Delta t v_x \frac{\partial \hat{u}_{m-1}}{\partial x} + \Delta t f\left(\mathbf{x}, t, \hat{u}_{m-1}\right). \tag{13}$$

This is a commonly used explicit time-stepping strategy that approximates $u(\mathbf{x}, t_m)$ by using $u(\mathbf{x}, t_{m-1})$. The right-hand side of (13) includes derivatives of $\hat{u}$ at $t = t_{m-1}$. Thus, to evaluate $u(\mathbf{x}, t_m)$, we need only find a suitable approximation to the derivatives. This will be done through RBF interpolation in next section.

3.2. RBFCM for approximation of the derivative functions

We will first interpolate the given concentration of oxidant and contaminant at previous time step $u(\mathbf{x}, t_{m-1})$ by RBFs. Then the unknown terms in (13), $\partial \hat{u}_{m-1}/\partial x$, $\partial^2 \hat{u}_{m-1}/\partial x^2$, and $\partial^2 \hat{u}_{m-1}/\partial y^2$ can be approximated in terms of the concentrations at the previous step t_{m-1}. Since RBFs are used to deal the spatial variables at the 'previous' time step only, we will omit the time variables t_{m-1} in the following derivations in this subsection. For simplicity, we use the transformation $v(\mathbf{x}) := u(\mathbf{x}, t_{m-1})$.

We begin by introducing some basic features of RBFs. We denote a set of scattered data in the domain by $X := \{\mathbf{x}_1, \mathbf{x}_2, \ldots, \mathbf{x}_N\} \in \Omega$, where N represents the number of points. The standard RBFCM uses an N-dimensional trial space of functions spanned by a kernel ϕ with respect to the point set X. Let $\mathbf{R}^2$ be a 2-dimensional Euclidean space. Let $\mathbf{x}_c \in \mathbf{R}^2$ and $\phi : \mathbf{R}^2 \to \mathbf{R}$ be an invariant function whose value at any point $\mathbf{x} \in \mathbf{R}^2$ depends only on the distance from the fixed point $\mathbf{x}_c$, and can be written as

$$\phi(\|\mathbf{x} - \mathbf{x}_c\|), \tag{14}$$

where $\|\cdot\|$ indicates the Euclidean norm. Then the function ϕ is a radial basis function, where $\mathbf{x}_c$ is the center of ϕ. The variable $r = \|\mathbf{x} - \mathbf{x}_c\|$ is often used in RBFs, and so is adopted in this study. Several commonly used RBFs are multiquadrics (MQ), inverse multiquadrics, Gaussian, thin-plate splines, polyharmonic splines, etc. MQ RBF has been proven to have a high-order rate of convergence. Thus, in this paper we use MQ

$$\phi(r) = \sqrt{r^2 + c^2}, \tag{15}$$

where $c > 0$ is called a shape parameter. The RBF shape parameter in MQ plays a major role in improving the accuracy of numerical solutions [28–32]. In general, the optimal shape parameter depends on the densities and distributions of the scattered nodes, and the function values at the nodes.

In the collocation method, the value of derivatives of $v(\mathbf{x})$ at each node $\mathbf{x}_i$, $i = 1, 2, \ldots, N$, is approximated by the values at the nodal points $v(\mathbf{x})$. From the time stepping method, the concentration, $v(\mathbf{x}_i)$, is known at every node $\mathbf{x}_i$. To

Please cite this article in press as: G. Yao, et al., Radial basis function simulation of slow-release permanganate for groundwater remediation via oxidation, Journal of Computational and Applied Mathematics (2016), http://dx.doi.org/10.1016/j.cam.2016.02.006

approximate the derivatives of $v(\mathbf{x}_i)$, we interpolate $v(\mathbf{x})$ on Ω using RBFs $\phi(r)$ with different centers $\mathbf{x}_k,\ k = 1, 2, \ldots, N$. Thus, we have

$$v(\mathbf{x}_j) = \sum_{k=1}^{N} \phi(\|\mathbf{x}_j - \mathbf{x}_k\|)\alpha_k, \quad j = 1,\ 2,\ \ldots,\ N. \tag{16}$$

This is an N by N system of linear equations:

$$\begin{bmatrix} v(\mathbf{x}_1) \\ v(\mathbf{x}_2) \\ \vdots \\ v(\mathbf{x}_N) \end{bmatrix} = \begin{bmatrix} \phi(\|\mathbf{x}_1 - \mathbf{x}_1\|) & \phi(\|\mathbf{x}_1 - \mathbf{x}_2\|) & \cdots & \phi(\|\mathbf{x}_1 - \mathbf{x}_N\|) \\ \phi(\|\mathbf{x}_2 - \mathbf{x}_1\|) & \phi(\|\mathbf{x}_2 - \mathbf{x}_2\|) & \cdots & \phi(\|\mathbf{x}_2 - \mathbf{x}_N\|) \\ \vdots & \vdots & \vdots & \vdots \\ \phi(\|\mathbf{x}_N - \mathbf{x}_1\|) & \phi(\|\mathbf{x}_n - \mathbf{x}_2\|) & \cdots & \phi(\|\mathbf{x}_N - \mathbf{x}_N\|) \end{bmatrix} \begin{bmatrix} \alpha_1 \\ \alpha_2 \\ \vdots \\ \alpha_N \end{bmatrix}. \tag{17}$$

It can be written in matrix notation as

$$\mathbf{v} = \mathbf{M}\boldsymbol{\alpha}, \tag{18}$$

where $\boldsymbol{\alpha} = [\alpha_1, \alpha_2, \ldots, \alpha_N]^T$ and $M_{jk} = \phi(\|\mathbf{x}_j - \mathbf{x}_k\|)$ is the jth row and the kth column entry of the matrix $\mathbf{M}$, and

$$\mathbf{v} = [v(\mathbf{x}_1), v(\mathbf{x}_2), \ldots, v(\mathbf{x}_N)]^T. \tag{19}$$

The unknown coefficients, $\boldsymbol{\alpha}$, can be obtained by inverting the matrix in Eq. (18), i.e.,

$$\alpha_k = \sum_{j=1}^{N} M_{kj}^{-1} v(\mathbf{x}_j), \quad k = 1,\ 2,\ \ldots,\ N. \tag{20}$$

Note that M_{kj}^{-1} is the kth row and jth column element of inverse matrix, $\mathbf{M}^{-1}$. Thus,

$$\hat{v}(\mathbf{x}) = \sum_{k=1}^{N} \phi(\|\mathbf{x} - \mathbf{x}_k\|) \sum_{j=1}^{N} M_{kj}^{-1} v(\mathbf{x}_j). \tag{21}$$

It is clear that the N-dimensional trial space of functions spanned by a kernel ϕ with respect to a point set X is reparametrized in terms of nodal values via the inverse of the kernel matrix M with entries $\phi(\mathbf{x}_j, \mathbf{x}_k),\ 1 \le j, k \le N$.

From Eqs. (15) and (16), we have

$$\mathbf{D}v(\mathbf{x}_i) = \sum_{k=1}^{N} \mathbf{D}\phi(\|\mathbf{x}_i - \mathbf{x}_k\|)\alpha_k, \tag{22}$$

where $\mathbf{D}$ is a differential operator. By direct differentiation,

$$\frac{\partial \phi(r)}{\partial x} = \frac{x}{\sqrt{r^2 + c^2}}, \qquad \frac{\partial \phi(r)}{\partial y} = \frac{y}{\sqrt{r^2 + c^2}}, \tag{23}$$

$$\frac{\partial^2 \phi(r)}{\partial x^2} = \frac{y^2 + c^2}{(r^2 + c^2)^{3/2}}, \qquad \frac{\partial^2 \phi(r)}{\partial y^2} = \frac{x^2 + c^2}{(r^2 + c^2)^{3/2}}. \tag{24}$$

As a result,

$$\frac{\partial v(\mathbf{x})}{\partial x} = \sum_{k=1}^{N} \frac{\partial \phi(\|\mathbf{x}_i - \mathbf{x}_k\|)}{\partial x} \left(\sum_{j=1}^{N} M_{jk}^{-1} v(\mathbf{x}_j) \right), \qquad \frac{\partial v(\mathbf{x})}{\partial y} = \sum_{k=1}^{N} \frac{\partial \phi(\|\mathbf{x}_i - \mathbf{x}_k\|)}{\partial y} \left(\sum_{j=1}^{N} M_{jk}^{-1} v(\mathbf{x}_j) \right), \tag{25}$$

$$\frac{\partial^2 v(\mathbf{x})}{\partial x^2} = \sum_{k=1}^{N} \frac{\partial^2 \phi(\|\mathbf{x}_i - \mathbf{x}_k\|)}{\partial x^2} \left(\sum_{j=1}^{N} M_{jk}^{-1} v(\mathbf{x}_j) \right), \qquad \frac{\partial^2 v(\mathbf{x})}{\partial y^2} = \sum_{k=1}^{N} \frac{\partial^2 \phi(\|\mathbf{x}_i - \mathbf{x}_k\|)}{\partial y^2} \left(\sum_{j=1}^{N} M_{jk}^{-1} v(\mathbf{x}_j) \right). \tag{26}$$

Then the unknown terms in (13), $\partial \hat{u}_{m-1}/\partial x$, $\partial^2 \hat{u}_{m-1}/\partial x^2$, and $\partial^2 \hat{u}_{m-1}/\partial y^2$ are approximated in terms of the concentrations at the previous step t_{m-1}, $u(\mathbf{x}_j, t_{m-1}),\ j = 1, 2, \ldots, N$. Then Eq. (13) gives an approximation of $u(\mathbf{x}_i, t_m)$ using Eq. (27):

$$\begin{aligned} \hat{u}_m(\mathbf{x}_i) = \hat{u}_{m-1}(\mathbf{x}_i) &+ \Delta t D_x \sum_{k=1}^{N} \frac{\partial^2 \phi(\|\mathbf{x}_i - \mathbf{x}_k\|)}{\partial x^2} \left(\sum_{j=1}^{N} M_{jk}^{-1} \hat{u}_{m-1}(\mathbf{x}_j) \right) \\ &+ \Delta t D_y \sum_{k=1}^{N} \frac{\partial^2 \phi(\|\mathbf{x}_i - \mathbf{x}_k\|)}{\partial y^2} \left(\sum_{j=1}^{N} M_{jk}^{-1} \hat{u}_{m-1}(\mathbf{x}_j) \right) \\ &- \Delta t v_x \sum_{k=1}^{N} \frac{\partial \phi(\|\mathbf{x}_i - \mathbf{x}_k\|)}{\partial x} \left(\sum_{j=1}^{N} M_{jk}^{-1} \hat{u}_{m-1}(\mathbf{x}_j) \right) + \Delta t f\left(\mathbf{x}_i, t_{m-1}, \hat{u}_{m-1}\right). \end{aligned} \tag{27}$$

Please cite this article in press as: G. Yao, et al., Radial basis function simulation of slow-release permanganate for groundwater remediation via oxidation, Journal of Computational and Applied Mathematics (2016), http://dx.doi.org/10.1016/j.cam.2016.02.006

3.3. Solution procedure for the proposed model

In this section, the solution procedure to approximate spatial–temporal concentrations is presented. The coupled system of PDEs is solved by the following steps:

1. Set the initial conditions and boundary conditions at the domain nodes;
2. Solve the diffusion–reaction equations for each time-step (e.g., from t_{m-1} to t_m):
   2.1 Calculate the weights, $\boldsymbol{\alpha}^1 = \sum_{j=1}^{N} M_{jk}^{-1} C_{m-1}^1(\mathbf{x}_j)$ and $\boldsymbol{\alpha}^2 = \sum_{j=1}^{N} M_{jk}^{-1} C_{m-1}^2(\mathbf{x}_j)$;
   2.2 Calculate the reaction term;
   2.3 Approximate the derivatives of C^1, C^2 at t_{m-1};
   2.4 Use the initial conditions to approximate C^1 and C^2 at t_m using Eq. (27);
   2.5 Update C^1 and C^2 with the concentrations at t_m;
3. Repeat Step 2.

Since we used a global RBFCM, there is a full matrix M of dimension $N \times N$ that needs to be inverted. The positive definiteness of MQ RBF guarantees the existence of the inverse matrix. Since the weights depend only on the locations of the scattered data and are time-independent, the inverse matrix M^{-1} can be pre-computed and stored before the iteration. Then we will need to find the weights in every time step $\boldsymbol{\alpha}^1$ for C^1 and $\boldsymbol{\alpha}^2$ for C^2.

The most time-consuming parts of the procedure are Steps 2 and 3 because the solutions of the diffusion–reaction equations have to be iteratively updated. To find the steady-state solution to the system of PDEs, the following convergence criterion may be used: $\max |u(\mathbf{x}, t_m) - u(\mathbf{x}, t_{m-1})| \leq \epsilon$, where ϵ is chosen as the steady-state convergence margin. However, all the simulations in this paper were conducted for a fixed time period $t \in [0, 100]$ days if it is not less. Thus, the computational cost will depend on the time-step size. In explicit time stepping methods, a small sampling distance in space generally implies the need for a small time-step, which apparently results in slow convergence. However, large time-steps often lead to diverging or oscillating numerical results. A good choice of time-step size can improve the rate of convergence and the stability as well. On the other hand, an explicit time discretization form is only conditionally stable and the stability analysis for diffusion equations yields the following Courant–Friedrichs–Lewy condition [33]: $\mu \Delta t / h^2 \leq 1/2$, where μ is the diffusion coefficients of oxidant and contaminant in the present work, Δt is the time-step size, and h is the grid distance. The above requirement is equivalent to: $\Delta t \leq h^2/2\mu$. In our explicit time-stepping strategy, the minimum grid distance $h = 0.3$ ft has been used. Due to the slow release rate $D_x = 0.01$ and $D_y = 0.001$, the time-step size restriction is very flexible. All numerical results are performed using FORTRAN90 on virtual machine running with a single CPU and 2 GB of ram. The host is an IBM HS20 blade server with Intel Xeon E5-2640 CPU's running at 2.5 GHz.

4. Numerical results

The purpose of the numerical study is to understand the impact of the slow-release cylinders on the contaminated domain and provide guidance to practitioners in the development of remediation strategies. To this end, we pose a suite of numerical experiments using the simulation tool to determine a zone of influence around a single cylinder and then consider the interaction of multiple cylinders. A domain of $\beta\%$ influence of the oxidant is defined by

$$\Omega_{\beta\%} = \{(x, y) \in \Omega : C^2(x, y) < \beta\% C_0^2(x, y)\}.$$

We use $\Omega_{70\%}$ to measure the level of the effectiveness of the cylinders. To distinguish the effectiveness of different experiments, we look at the average contaminant concentration over time:

$$\overline{C}^1 = \frac{1}{N} \sum_{i=1}^{N} C_i^1, \qquad \overline{C}^2 = \frac{1}{N} \sum_{i=1}^{N} C_i^2,$$

where N is the total number of points in the domain.

4.1. Physical setting

Our hydrological settings are homogeneous rectangles of 13 ft by 3 ft, 13 ft by 6 ft or 26 ft by 6 ft. The physical constants and parameters are summarized in Table 1. The source term in Eq. (1) is the oxidant release from the cylinder. The concentration of the oxidant at the source is described in [12]. Fig. 3 shows the oxidant release from the cylinders generated by Carus Corporation from day 0 to day 100. We use cubic splines to evaluate the source at the intermediate times. To observe the effect of oxidant at different times and locations, we use six observation points downstream of the installed cylinders at (2.6, 1.5), (2.925, 1.5), (3.9, 1.5), (4.875, 1.5), (7.15, 1.5), and (12.025, 1.5) ft, see Fig. 2.

4.2. Results

We perform a suite of numerical experiments to understand the placement and interactions of cylinders over time. Specifically, we determine the domain of influence for up to three cylinders; we numerically estimate the optimal placement of a total of two cylinders in the domain; and we examine performance of a total of three cylinders with various installation locations and times of the third cylinder.

Please cite this article in press as: G. Yao, et al., Radial basis function simulation of slow-release permanganate for groundwater remediation via oxidation, Journal of Computational and Applied Mathematics (2016), http://dx.doi.org/10.1016/j.cam.2016.02.006

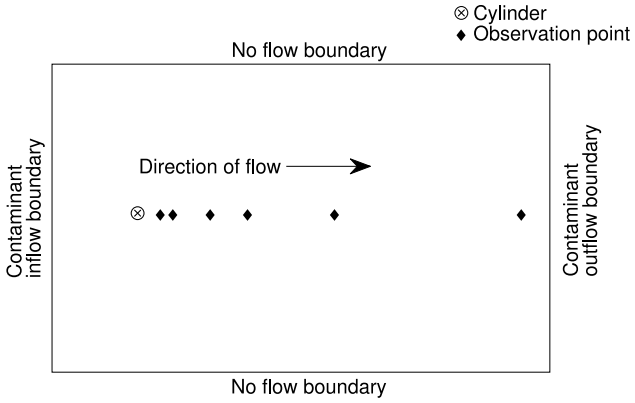

Fig. 2. Physical setting of the model.

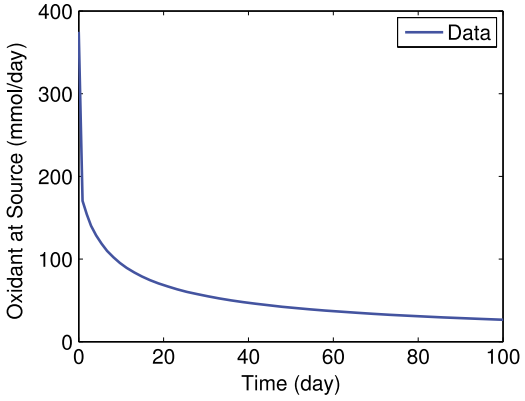

Fig. 3. Oxidant level C^1 at the source point.

Table 1
Physical parameters used in this paper.

Value	Unit	Symbol/name
119	mg/mmol	Molecular weight of oxidant
6	mg/L	Initial concentration of contaminant
1	Unitless	Retardation factor for contaminant
1	Unitless	Retardation factor for oxidant
0.01	ft^2/day	D_x
0.001	ft^2/day	D_y
0.340157491	ft/day	v_x
88.11	mg/mmol	Molecular weight of contaminant
0.00435456	L/mmol-day	Reaction constant
13	ft	L_x
3 or 6	ft	L_y
0.104166667	ft	Cylinder radius
6	Unitless	Number of observation points
1,4-dioxane	Unitless	Contaminant type

4.2.1. Number and placement of the cylinders

Case 1. Single cylinder

Consider a single cylinder fixed at (1.95, 1.5) ft. A total of 447 points are uniformly distributed in the domain and used in the RBF method. Time step size is chosen as $\Delta t = 0.002$ days. It takes about 102 s for a simulation time of 100 days. Figs. 4 and 5 show the oxidant and the contaminant concentration at six different observation points downside of the stream. Notice that the oxidant concentration at observation points close to the cylinder behaves as expected (similar to the source model). Further away from the cylinder, there is less oxidant present when it reaches the observation points, so it has less impact on the contaminant (see the lower-right figures). During the simulation, we keep track of the percentage of the domain that is lower than 70% of the original contaminant concentration to determine when the maximum area of the domain of influence is met. At $t = 30$ days, the oxidant reaches the maximum domain of 70% influence. The

Please cite this article in press as: G. Yao, et al., Radial basis function simulation of slow-release permanganate for groundwater remediation via oxidation, Journal of Computational and Applied Mathematics (2016), http://dx.doi.org/10.1016/j.cam.2016.02.006

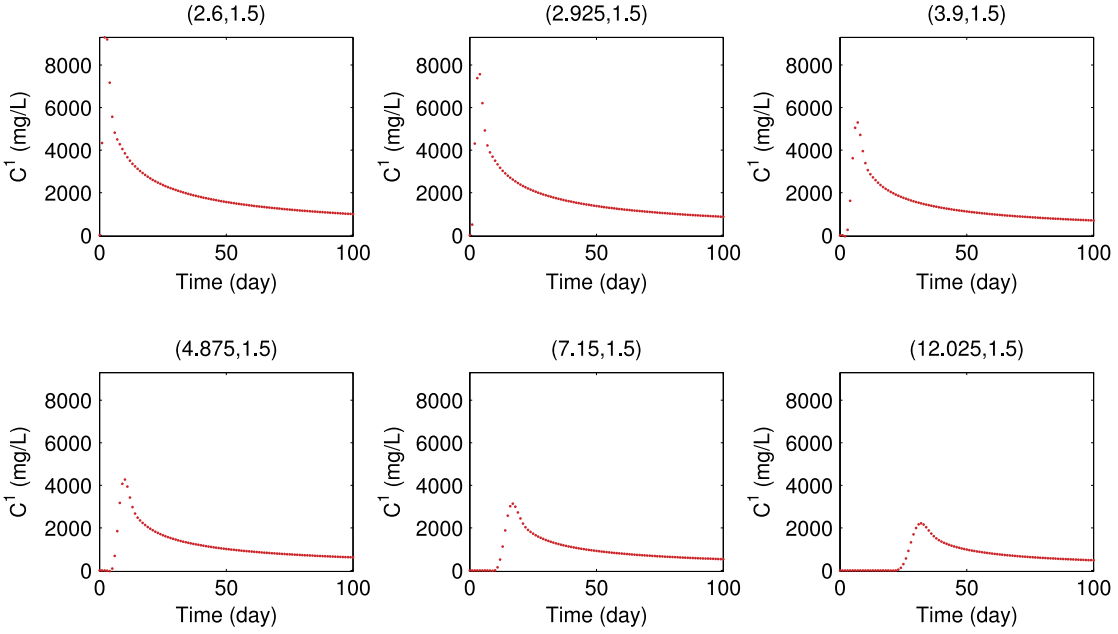

Fig. 4. Oxidant concentration with one source located at (1.95, 1.5) ft at six different observation points over time.

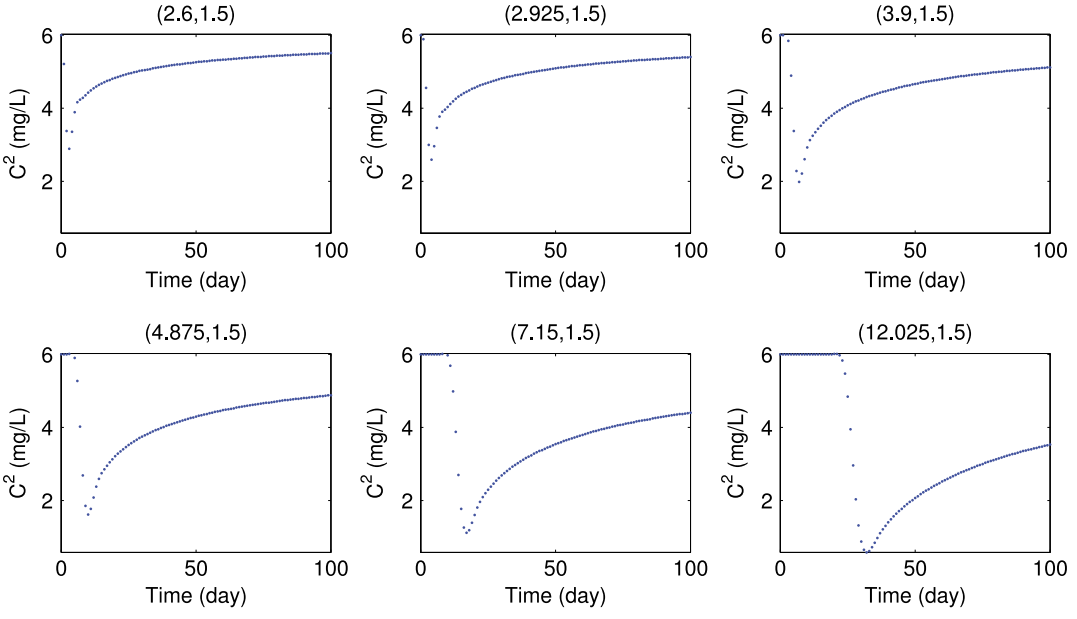

Fig. 5. Contaminant concentration with one source located at (1.95, 1.5) ft at six different observation points over time.

contaminant concentration on 31.32% of the domain, 12.2148 ft^2, decreases to 70% of the initial contaminant. Figs. 6 and 7 show the oxidant and contaminant concentration profile at different times. These profiles are consistent with the work from Wolf (2013) [12] and Slaugh (2015) [13]. It illustrates the effect of lateral diffusion on the amount of the oxidant present, which warrants further investigation in the presence of two cylinders.

Case 2. Two cylinders

For this study, we consider two cylinders and the impact of the distance between them on the domain of influence. For this reason, we consider a larger domain 13 ft by 6 ft. A total of 857 points are uniformly distributed in the domain and used in the RBF method. We increase the time step size for efficiency, so it took only 41 s for a simulation time of 100 days. We increase the vertical distance between two cylinders and determine the time and maximum area of the domain of 70% influence. Table 2 shows these values. From **Case 1** we saw the impact of the diffusion was within a 3 ft distance for one cylinder. Table 2 shows that as the distance between them increases to 2.4 ft, the maximum area also

Please cite this article in press as: G. Yao, et al., Radial basis function simulation of slow-release permanganate for groundwater remediation via oxidation, Journal of Computational and Applied Mathematics (2016), http://dx.doi.org/10.1016/j.cam.2016.02.006

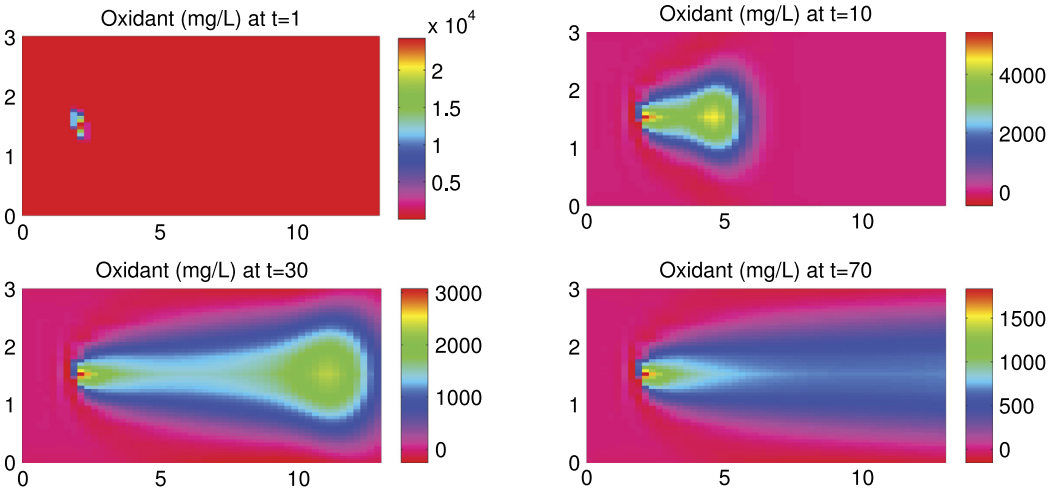

Fig. 6. Oxidant concentration profile with one source located at (1.95, 1.5) ft at four different observation times.

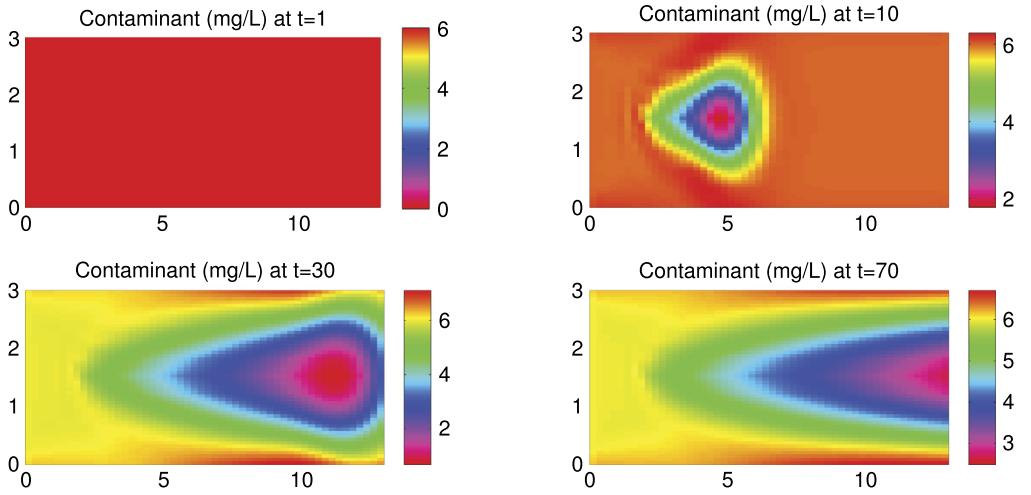

Fig. 7. Contaminant concentration profile with one source located at (1.95, 1.5) ft at four different observation times.

Table 2
Impact of the placement of two cylinders in the vertical direction.

Cyl 1 (ft)	Cyl 2 (ft)	Distance (ft)	Time (days)	Area (ft^2)	Percent of domain
(1.95, 2.4)	(1.95, 3.6)	1.2	30	26.8494	34.42%
(1.95, 2.1)	(1.95, 3.9)	1.8	32	29.3936	37.69%
(1.95, 1.8)	(1.95, 4.2)	2.4	31	30.6721	39.32%

increases, implying the optimal distance is between 2.4 and 3 ft. Note that our conclusion only holds for this test case. The domain of interests is chosen so it is large enough to find out the domain of influence of the placed cylinders. The source term in Fig. 14 is from our experimental data, while the oxidant releases from the cylinders that are produced by Carus Corporation. Currently, we are tasked to give a general guidance on how to place these cylinders so we can reach maximum oxidant effect from the cylinders. In fact, validation the model with experimental data is part of our future work plan.

We repeat this experiment by changing the horizontal distance between the two cylinders. For this reason, we consider an even larger domain 26 ft by 6 ft. We fixed cylinder one at (1.93, 3) ft and consider seven locations for the second cylinder downstream of the first one. Those locations, the time taken to reach the maximum domain of 70% influence, the corresponding area, and the percentage of the domain are shown in Table 3.

Note that having the second cylinder closer to the first cylinder appears the best results in terms of the largest domain of influence, although it takes longer to reach that. However, the design objective is to have the largest area of oxidant coverage over a long time horizon.

Please cite this article in press as: G. Yao, et al., Radial basis function simulation of slow-release permanganate for groundwater remediation via oxidation, Journal of Computational and Applied Mathematics (2016), http://dx.doi.org/10.1016/j.cam.2016.02.006

Table 3
Impact of the placement of two cylinders in the horizontal direction.

Cyl 1 (ft)	Cyl 2 (ft)	Distance (ft)	Time (days)	Area (ft^2)	Percent of domain
(1.95, 3)	(3.25, 3)	1.30	63	97.9323	62.78%
(1.95, 3)	(5.85, 3)	3.90	57	93.5636	59.98%
(1.95, 3)	(7.80, 3)	5.85	51	93.1995	59.74%
(1.95, 3)	(10.40, 3)	8.45	67	86.4644	55.43%
(1.95, 3)	(11.05, 3)	9.10	62	86.4644	55.43%
(1.95, 3)	(13.00, 3)	11.05	62	84.6441	54.26%
(1.95, 3)	(17.55, 3)	15.60	63	83.1879	53.33%

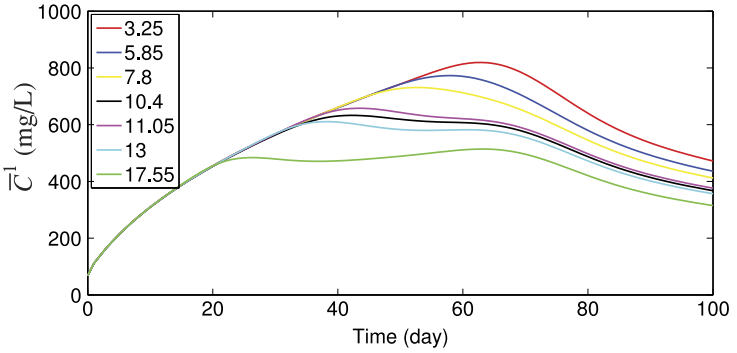

Fig. 8. Oxidant concentrations when one cylinder is located at (1.95, 3) ft and the other is located at $y = 3$ ft with various x locations over time.

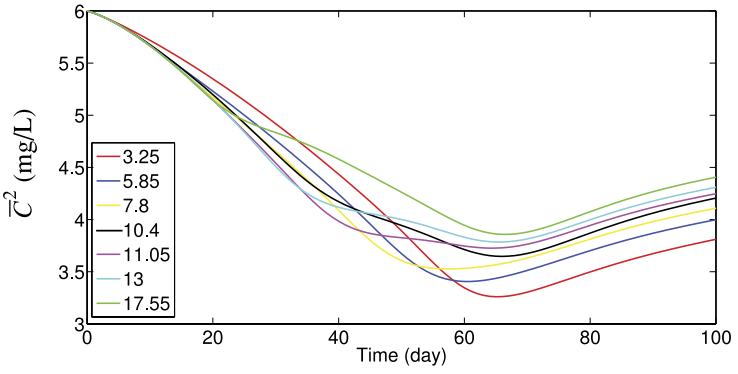

Fig. 9. Contaminant concentrations when one cylinder is located at (1.95, 3) ft and the other is located at $y = 3$ ft with various x locations over time.

We also show the average oxidant and contaminant concentrations over time for these experiments, see Figs. 8 and 9. As the second cylinder is placed further away, more oxidant is leaving the right side boundary, so less is present. For the initial times, the cylinders spaced further away, give an overall better results before a certain time (roughly around 57 days), but as time progresses past this point, it appears having the second cylinder closer is more beneficial.

To gain insight, consider the percentage of the domain of 70% influence over time for the four best cases, see Fig. 10. Here we can see having the cylinder at $x = 10.40$ ft, $y = 3$ ft yields a much cleaner region up until roughly 41 days, and does not change more than approximately 10% for the next 60 days. These experiments imply placing the second cylinder further down stream achieves peak percentage of domain in $\Omega_{70\%}$ sooner and plateaus losing only about 10% of the domain over the remaining time in the simulation.

Case 3. Three source points

To understand the impact of the third cylinder, we fix two cylinders at (1.95, 1.8) and (1.95, 4.2) in a domain of 26 ft by 6 ft, and consider an additional cylinder with three possible locations and four possible installation times for total of twelve experiments. It takes about 58 s to simulate one experiment. Table 4 shows all of the experiments. Exp.6 indicates that the third cylinder is installed at location (10, 3) at day 27, see Fig. 11.

We tabulated the percent of the domain with contaminant less than 70% of the initial contaminant concentration. Lines of the same color represents that the third cylinder is installed at the same location but at different times. From Fig. 12, we see that the third cylinder installed at location (10.4, 30) at day 0 is the most efficient in terms of the domain of 70% influence. All of the experiments on installing the third cylinder at days other than day 0 generate a very similar domain

Table 4
Different simulation cases for the third cylinder.

Time (days)/location (ft)	(8.45, 3)	(10.4, 3)	(11.5, 3)
0	Exp.1	Exp.5	Exp.9
27	Exp.2	Exp.6	Exp.10
31	Exp.3	Exp.7	Exp.11
35	Exp.4	Exp.8	Exp.12

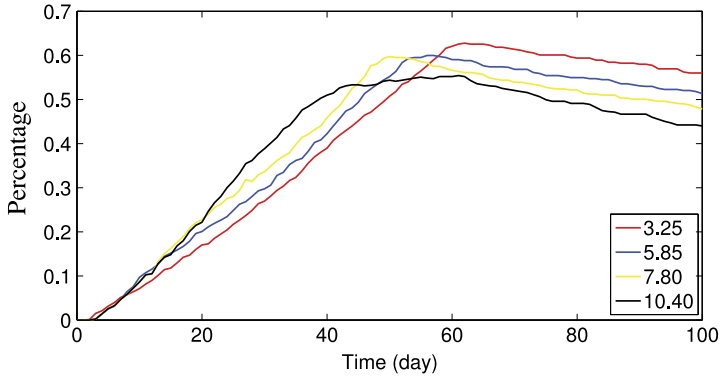

Fig. 10. Percentage of domain in $\Omega_{70\%}$ influence over time.

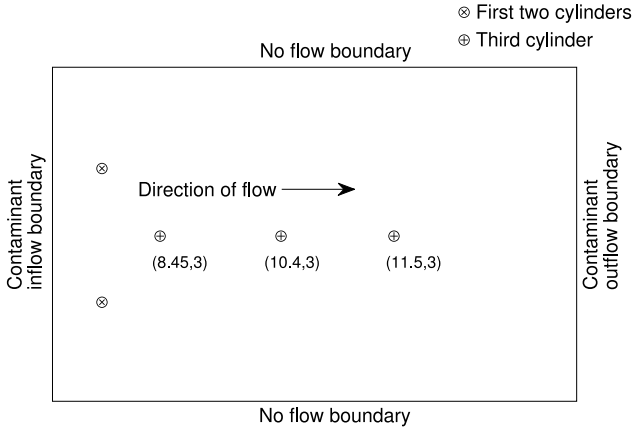

Fig. 11. Physical setting of the three cylinder model.

of influence. From Figs. 12–14, we see that a slightly better result appears when we place the third cylinder at location (8.45, 3) in terms of the average concentrations. These experiments suggest the optimal location for the third cylinder is between 8 and 10 ft.

5. Conclusion

We have used radial basis functions to simulate coupled reactive transport in the context of remediation. The underlying model is a system of nonlinear partial differential equations that describes the interaction of a MnO_4^- cylinder with a contaminant in the saturated subsurface. The velocity we used in this system of PDEs is being calculated using hydraulic head gradients and conductivities. So it is a general PDE with many applications but porous media transport is one in this context. In addition, the coupled NOD model is specified by the soil type and included to represent bioremediation in porous media. The model provides guidance in terms of understanding the placement and interaction of cylinders. We used several metrics including a domain of influence in which the amount of contaminant present is less than a certain percentage of the initial concentration. Our results indicate that cylinders should be place between 2.4 and 3 ft apart vertically and that subsequent cylinders downstream should be roughly 8–10 ft downstream. These results are specific to the site groundwater velocity, natural oxidant demand, contaminant type, and contaminant concentration used for these simulations and as shown in Table 1. Results would vary as these site conditions vary.

The framework used here is flexible in that physical model parameters can easily be modified to understand the system design for other hydrological settings. Our focus in this manuscript is to use simple tools developed in the sciences (the global

Please cite this article in press as: G. Yao, et al., Radial basis function simulation of slow-release permanganate for groundwater remediation via oxidation, Journal of Computational and Applied Mathematics (2016), http://dx.doi.org/10.1016/j.cam.2016.02.006

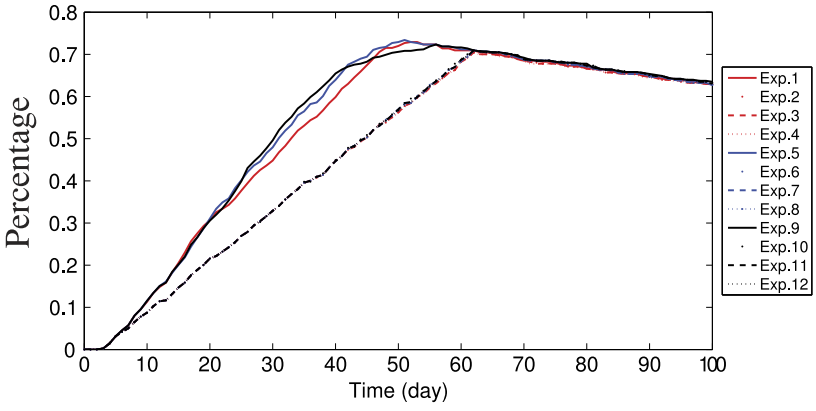

Fig. 12. Percentage of the domain with contaminant less than 70% of the initial contaminant concentration when two cylinders are installed at (1.95, 1.8) and (1.95, 4.2) and the third cylinder is injected at different locations and times, as listed in Table 4. (For interpretation of the references to color in this figure legend, the reader is referred to the web version of this article.)

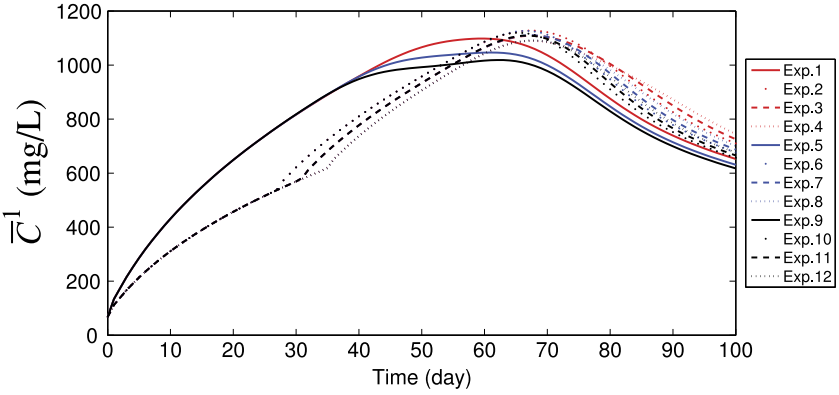

Fig. 13. Average oxidant concentration when two cylinders are installed at (1.95, 1.8) and (1.95, 4.2) and the third cylinder is injected at different locations and times, as listed in Table 4. (For interpretation of the references to color in this figure legend, the reader is referred to the web version of this article.)

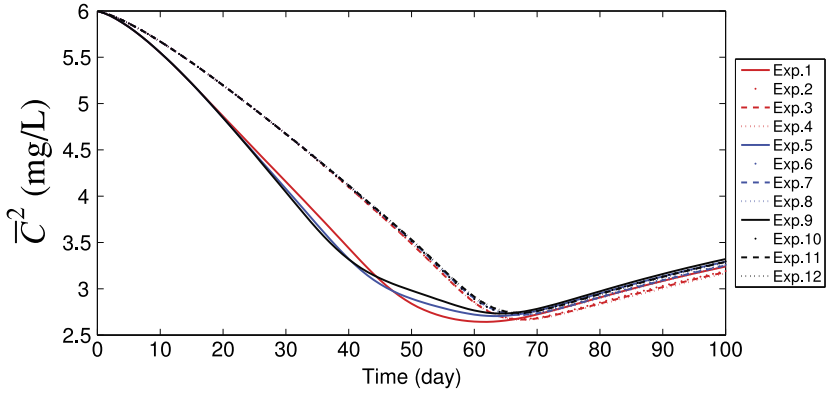

Fig. 14. Average contaminant concentration when two cylinders are installed at (1.95, 1.8) and (1.95, 4.2) and the third cylinder is injected at different locations and times, as listed in Table 4. (For interpretation of the references to color in this figure legend, the reader is referred to the web version of this article.)

method with the system of transport equations) to validate the real word applications for industry partners. The use of RBFs also means that locations of cylinders are not tied to a grid. With existing numerical method on this PDE model, we were able to make many useful suggestions to help guide with the use of this emerging remediation tool, the oxidant cylinder. We were able to advise Carus Corporation on how to design more efficient and effective contaminant treatment tools. The next step in this work is to model installation and replacement costs. Such models can be paired with optimization algorithms to understand efficient design strategies for large-scale clean-up sites. In particular, this work has provided initial insight

Please cite this article in press as: G. Yao, et al., Radial basis function simulation of slow-release permanganate for groundwater remediation via oxidation, Journal of Computational and Applied Mathematics (2016), http://dx.doi.org/10.1016/j.cam.2016.02.006

that will assist in the development of constraints on the placements of a network of cylinders over a larger domain. We may need a more robust local RBF method for such purpose with more complicate dispersion relation in the PDE model.

Acknowledgment

The authors would like to acknowledge funding for this work from the Environmental Security Technology Certification Program (ESTCP), Project ER-201324, "Sustained In Situ Chemical Oxidation (ISCO) of 1,4-Dioxane Using Slow Release Chemical Oxidant Cylinders".

References

[1] E.S. Lee, F.W. Schwartz, Characteristics and applications of controlled-release $KMnO_4$ for groundwater remediation, Chemosphere 66 (11) (2007) 2058–2066.
[2] M.D. Christenson, A. Kambhu, S.D. Comfort, Using slow-release permanganate candles to remove TCE from a low permeable aquifer at a former landfill, Chemosphere 89 (6) (2012) 680–687.
[3] A. Kambhu, S. Comfort, C. Chokejaroenrat, Developing slow-release persulfate candles to treat BTEX contaminated groundwater, Chemosphere 89 (6) (2012) 656–664.
[4] N. Kang, I. Hua, P. Suresh, C. Rao, Production and characterization of encapsulated potassium permanganate for sustained release as an in situ oxidant, Ind. Eng. Chem. Res. 43 (17) (2004) 5187–5193.
[5] L. Rauscher, C. Sakulthaew, S. Comfort, Using slow-release permanganate candles to remediate PAH-contaminated water, J. Hazard Mater. 241–242 (2012) 441–449.
[6] C. Ross, L.C. Murdoch, D.L. Freedman, Characteristics of potassium permanganate encapsulated in polymer, J. Environ. Eng. 131 (8) (2005) 1203–1211.
[7] P.V. Brady, C.M. Bethke, Beyond the Kd approach, Ground Water 38 (2000) 321–322.
[8] P.C. Lichtner, Contiuum model for simultaneous chemical reactions and mass transport in hydrothermal systems, Geochem. Cosmochem. Acta 49 (1985) 779–800.
[9] M. Gharasoo, F. Centler, P. Regnier, H. Harms, M. Thullner, A reactive transport modelling approach to simulate biogeochemical processes in pore structures with pore-scale heterogeneities, Environ. Modell. Softw. 30 (2012) 102–114.
[10] C.I. Steefel, A.C. Lasaga, A coupled model for transport of multiple chemical species and kinetic precipitation/dissolution reactions with application to reactive flow in single phase hydrothermal systems, Amer. J. Sci. 294 (1994) 529–592.
[11] G.T. Yeh, V.S. Tripathi, A critical evaluation of recent developments in hydrogeochemical transport models of reactive multi-chemical components, Water Resour. Res. 25 (1989) 93–108.
[12] G. Wolf, Slow release permanganate cylinders for sustainable in situ chemical oxidation: Development of a conceptual design tool (M.S. Thesis), Clarkson University, Potsdam, NY, 2013.
[13] E. Slaugh, Design tool for slow-release oxidant cylinders (Unpublished Honors Undergraduate Thesis), Clarkson University, Potsdam, NY, 2015.
[14] E.J. Kansa, Multiquadrics—a scattered data approximation scheme with applications to computational fluid-dynamics. 2. Solutions to parabolic, hyperbolic and elliptic partial–differential equations, Comput. Math. Appl. 19 (1990) 147–161.
[15] M. Zerroukat, H. Power, C.S. Chen, A numerical method for heat transfer problems using collocation and radial basis functions, Internat. J. Numer. Methods Engrg. 42 (1998) 1263–1278.
[16] B. Sarler, D. Gobin, B. Goyeau, J. Perko, H. Power, Natural convection in porous media-dual reciprocity boundary element method solution of the Darcy model, Int. J. Numer. Methods Fluids 33 (2000) 279–312.
[17] B. Sarler, A radial basis function collocation approach in computational fluid dynamics, Comput. Model. Eng. Sci. 7 (2005) 185–193.
[18] A.I. Tolstykh, D.A. Shirobokov, On using radial basis functions in a "finite difference" mode with applications to elasticity problems, Comput. Mech. 33 (2003) 68–79.
[19] P.H. Wen, C.S. Chen, The method of particular solutions for solving scalar wave equations, Int. J. Numer. Methods Biomed. Eng. 26 (2010) 1878–1889.
[20] La Rocca, H. Power, Free mesh radial basis function collocation approach for the numerical solution of system of multi-ion electrolytes, Internat. J. Numer. Methods Engrg. 64 (13) (2005) 1699–1734.
[21] J. Li, C.S. Chen, D. Peppery, Y. Chen, Mesh-free method for groundwater modeling, in: International Series on Advances in Boundary Elements, 2002.
[22] Y. Alhuri, D. Ouazar, A. Taik, Comparison between local and global Mesh-free methods for Ground-Water modeling, IJCSI Int. J. Comput. Sci. Issues 8 (2) (2011).
[23] S. Chantasiriwan, Performance of Multiquadric collocation method in solving lid-driven cavity flow problem with low Reynolds number, Comput. Model. Eng. Sci. 15 (2006) 137–146.
[24] Scott A. Sarra, A local radial basis function method for advection–diffusion–reaction equations on complexly shaped domains, Appl. Math. Comput. 218 (19) (2012) 9853–9865.
[25] Guangming Yao, Zeyun Yu, A localized meshless approach for modeling spatial–temporal calcium dynamics in ventricular myocytes, Int. J. Numer. Methods Biomed. Eng. 28 (2) (2012) 187–204.
[26] E.S. Lee, F.W. Schwartz, Characterization and optimization of long-term controlled release system for groundwater remediation: a generalized modeling approach, Chemosphere 69 (2) (2007) 247–253.
[27] T.J. Roseman, W.I. Higuchi, Release of medroxyprogesterone acetate from a silicone polymer, J. Pharm. Sci. 59 (3) (1970) 353–357.
[28] G.E. Fasshauer, Solving partial differential equations by collocation with radial basis functions, in: A.L. Mehaute, C. Rabut, L.L. Schumaker (Eds.), Surface Fitting and Multiresolution Methods, 1997, pp. 131–138.
[29] G.E. Fasshauer, J.G. Zhang, On choosing optimal shape parameters for RBF approximation, Numer. Algorithms 45 (2007) 345–368.
[30] C.-S. Huang, C.F. Lee, A.H.-D. Cheng, Error estimate, optimal shape factor, and high precision computation of multiquadric collocation method, Eng. Anal. Bound. Elem. 31 (7) (2007) 614–623.
[31] J.G. Wang, G.R. Liu, On the optimal shape parameters of radial basis functions used for 2-d meshless methods, Comput. Methods Appl. Mech. Engrg. 191 (2002) 2611–2630.
[32] J. Wertz, E.J. Kansa, L. Ling, The role of the multiquadric shape parameters in solving elliptic partial differential equations, Comput. Math. Appl. 51 (8) (2006) 1335–1348.
[33] R. Courant, K. Friedrichs, H. Lewy, On the partial difference equations of mathematical physics, IBM J. Res. Dev. 11 (2) (1967) 215–234.

Please cite this article in press as: G. Yao, et al., Radial basis function simulation of slow-release permanganate for groundwater remediation via oxidation, Journal of Computational and Applied Mathematics (2016), http://dx.doi.org/10.1016/j.cam.2016.02.006